Comparison Between the Oxidation Behaviors of Ti6242S, Ti6246, TiXT Alloys, and Pure Titanium

Benjamin Vincent, Virgil Optasanu, Frédéric Herbst, Sébastien Chevalier, Ioana Popa, Tony Montesin, Luc Lavisse

This is a working version of the paper published here : https://doi.org/10.1007/s11085-021-10051-w

Comparison between the Oxidation Behaviors of Ti6242S, Ti6246, TiXT Alloys and Pure Titanium

Benjamin VINCENT, Virgil OPTASANU, Frédéric HERBST, Sébastien CHEVALIER, Ioana POPA, Tony MONTESIN, Luc LAVISSE

ICB, UMR 6303 CNRS – Univ. Bourgogne Franche Comté, 21078 DIJON, France
benjamin_vincent@etu.u-bourgogne.fr ; virgil.optasanu@u-bourgogne.fr ; sebastien.chevalier@u-bourgogne.fr ; ioana.popa@u-bourgogne.fr ; tony.montesin@u-bourgogne.fr ; luc.lavisse@u-bourgogne.fr

Abstract. Isothermal oxidation tests were performed on Ti6242S (Ti - 6% Al – 2% Sn – 4% Zr – 2% Mo, 0.08% Si), Ti6246 (Ti - 6% Al – 2% Sn – 4% Zr – 6% Mo, 0.05% Si), TiXT (Ti - 0.45% Si) alloys and pure titanium in laboratory air at 560°C, 600°C and 650°C for 1000h to compare their oxidation behaviors. The study aims to highlight the role of molybdenum and silicon in the oxidation resistance of titanium alloys. The results show that 6 wt.% of Mo in Ti6246 alloys does not substantially change the oxidation behavior compared to Ti6242S alloy containing only 2 wt.% of Mo. Meanwhile, the presence of 0.45 wt.% Si seems to be clearly beneficial for the oxidation resistance, reducing the parabolic rate constant by a factor larger than 2 as compared to pure titanium.

Keywords Titanium alloys, high temperature oxidation, oxygen diffusion, kinetics

1. Introduction

Titanium alloys are widely used in aeronautic applications because of their low density compared to steel and their relative high strength, contributing to a reduction of pollutant emission. These alloys also have good oxidation resistance at moderate temperatures (<500°C) and can be used in aircraft parts exposed to hot atmospheres. This is the case for near alpha titanium alloys, which were developed in order to improve the high temperature oxidation resistance. One example is Ti6242S (Ti – 6% Al – 2% Sn – 4% Zr – 2% Mo, 0,08% Si) of which behavior was studied by several authors [1-8], IMI 834 [9], Ti1100 [10,11] or Ti60 [12].

A way to improve the oxidation resistance is the optimization of alloying elements in titanium alloys. Some alloying elements, like aluminum or silicon, can increase the oxidation resistance whereas others, like vanadium, can accelerate the oxidation kinetics and then lead to faster degradation. Tin and zirconium are found to be neutral for the oxidation behavior [13]. Aluminum allows the use of titanium alloys at higher temperatures and for longer periods of exposure, by lowering the oxidation rates [14]. Its presence leads to the formation of Al_2O_3 in the oxide layer, which helps to reduce the oxygen flux through the scale. The weight gain and the oxide scale growth are slower as compared to pure titanium. However, most of titanium alloys limit the presence of aluminum to 6 wt.% in order to avoid Ti_3Al phase formation, which degrades ductility [15]. Silicon is also beneficial for the oxidation resistance. It is shown that its addition can reduce the weight gain caused by oxidation [16,17]. It is shown that its presence can help to reduce the porosity of the oxide layer and increases its adherence. Silicon content is limited to 1 wt.% to avoid silicide precipitates, which cause embrittlement of the alloys. The effect of molybdenum in high temperature oxidation has been studied in Ti-Al alloys. Shida showed that 2-6 wt.% of Mo decrease the weight gain after 100h of exposure in air at temperatures between 800°C and 1000°C in Ti-35wt.%Al alloy [18]. The presence of 2 wt.% Mo in the alloy reduces the k_p value by a factor of 2 as compared with the composition from without Mo. However, no similar studies were found in near alpha titanium alloys.

This study has two goals. The first is to compare the oxidation behavior of commercial titanium alloys Ti6242S (Ti – 6%Al – 2% Sn, 4% Zr – 2% Mo – 0.08%Si) and Ti6246 (Ti – 6%Al – 2% Sn, 4% Zr – 6% Mo – 0.05%Si) in order to evaluate the influence of the molybdenum content on the high temperature oxidation. The second aim is to evaluate the role of silicon by comparing the TiXT alloy (Ti – 0.45% Si) for commercially pure titanium (99.6% of purity, grade 2). For the comparison, isothermal oxidation tests were performed up to 1000h at 560°C, 600°C and 650°C in laboratory air to discontinuously measure the weight gains and estimate the parabolic constants of each alloy. Scanning Electron Microscopy (SEM) was used to analyze the oxide scales morphologies and compositions and X-ray Diffraction (XRD) was used for crystalline phase identification. The oxygen diffusion zone was estimated by

microhardness testing for each temperature. The oxygen diffusion coefficient corresponding to oxygen dissolution in the substrates, the activation energy for oxygen diffusion and the activation energy for the overall oxidation are estimated by processing these data.

2. Experimental methods

The specimens were cut from parallelepiped rods in small plates of 10 x 10 x 1 mm^3. They were then mechanically polished on SiC grids up to P600 and cleaned with ethanol in ultrasonic bath for 10 minutes. The mass of each sample was measured with a Mettler Toledo balance with 0.1 mg accuracy. The dimensions were measured with a digital caliper with 10 µm accuracy.

The samples were isothermally oxidized in muffle furnace at 560°C, 600°C and 650°C in laboratory air up to 1000 h. Individual samples were extracted after 25, 50, 150, 300, 500, 800 and 1000 hours of high temperature exposure and the mass gain per surface area of each sample was measured. Some of the samples were doubled for reproducibility evaluation.
Crystalline phases present in the samples before and after oxidation were identified by X-ray diffraction in θ-θ geometry by using diffractometer Bruker D8 Discover with monochromatic Cu Kα radiation ($\lambda_{K\alpha 1}$ = 0.154156 nm) and equipped with LYNXEYE detector. The surface morphology and composition of the oxide scales were performed using JEOL JSM-7600F scanning electron microscope (SEM) equipped with Energy Dispersive X-Ray Spectroscopy (EDS). Cross-section SEM analyses were performed after preparation of the samples by gold sputtering, copper electrolytic deposition, cross cutting, polishing with ascending grid SiC paper and super-finishing with 30 nm colloidal silica suspension.

The oxygen dissolution zone in the oxidized samples was revealed by Vickers microhardness measurements using Zwick indenter with a load of 25 g applied for 10 seconds in each print. The distance from the interface oxide/metal of the indentation prints was measured with an optical microscope. 50 indentations were made for each profile, spacing the imprints in the depth direction by an increment of 1 µm for specimens oxidized at the lower exposure time, up to 5 µm for longer exposure time.

3. Results and discussion

3.1. Raw materials

The microstructures of the raw samples are presented in **Fig. 1**. Ti6242S is a near-α alloy with a small proportion of β phase. It has a bimodal structure with alpha grains about 20 µm. Ti6246 has a quite similar microstructure except that the higher content of beta-stabilizer molybdenum leads to larger proportion of beta phase. TiXT and pure Ti present similar microstructures, except that the alloy contains a very small proportion of β phase around the grain boundaries due to the presence of 0.45 wt.% of Si.

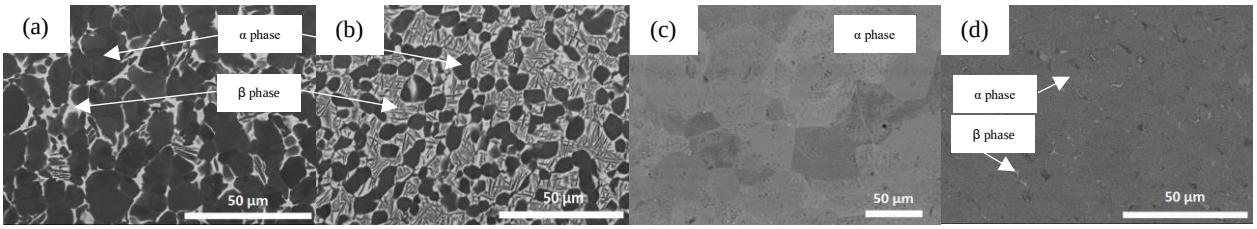

Fig. 1 SEM images of as received alloys microstructures of (a) Ti6242S, (b) Ti6246, (c) pure Ti and (d) TiXT

3.2. Oxidation kinetics

Fig. 2 presents the mass gain versus the time at 560°C, 600°C and 650°C for Ti6242S and Ti6246 alloys (**Fig. 2a**) and for pure Ti and TiXT alloy (**Fig. 2b**). For each alloy, the mass gain follows a parabolic curve, which means that diffusion is the limiting step and that the oxide formed during exposures at elevated temperatures is dense and protective. The temporal evolution of the normalized mass gain is described by [19]:

$$\left(\frac{\Delta m}{S}\right)^2 = k_p t$$

where Δm is the mass gain, S is the sample surface, k_p is the oxidation parabolic rate constant and t the exposure time. In this range of temperature, titanium alloys are known to undergo anionic oxidation process: O^{2-} ions diffuse through the oxide scale to form new oxides at the oxide/metal interface and to diffuse further into the metal. Indeed, it is well known that oxygen has high solubility in pure Ti up to 33 at. % [20,22].

Fig. 2 shows similar mass gains for Ti6242S and Ti6246 alloys for the three temperatures (560°C, 600°C and 650°C), but the difference of mass gain is clear between TiXT and pure titanium. For the three temperatures, the mass gain curve of pure titanium is always above the mass gain curve of TiXT, and the relative difference increases with the temperature.
The parabolic rate constants are calculated by plotting the normalized mass curve versus the square root of the time. The resulting k_p values are listed in **Table 1**. The lowest values of the parabolic rate constants are obtained for Ti6242S alloy. These values are slightly higher for Ti6246 for the three temperatures, but the difference is not significant, especially at the highest temperature where the difference is only of 3.7%. Higher amount of of Mo (6%) in Ti6246 alloy as compared to Ti6242S alloy (2%) does not seem to significantly change the mass gain during oxidation. No other studies were found to compare these results.
The difference between the unalloyed titanium and TiXT is larger for the normalized mass gain and the parabolic rate constants for all the temperatures. The oxidation parabolic rate constants are 1.8, 2.4 and 2.2 higher for pure titanium than for TiXT at 560°C, 600°C and 650°C, respectively. These results show that TiXT has clearly better resistance against high temperature oxidation.

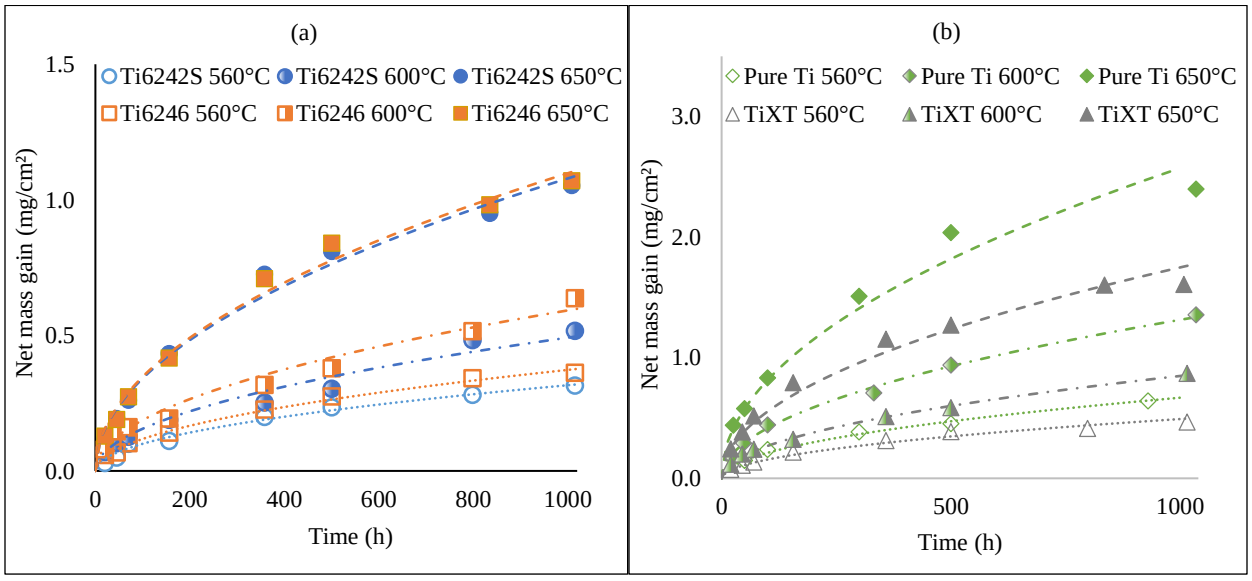

Fig. 2 Normalized net mass gain versus the time at 560°C, 600°C and 650°C for (a) Ti6242S / Ti6246, and (b) pure Ti / TiXT

Table 1
Calculated values of parabolic rate constants at 560°C, 600°C and 650°C for the overall weight gain up to 1000h

	k_p ($g^2.cm^{-4}.s^{-1}$)		
Alloy	560°C	600°C	650°C
Ti6242S	2.8×10^{-14}	6.7×10^{-14}	3.2×10^{-13}
Ti6246	3.9×10^{-14}	9.7×10^{-14}	3.3×10^{-13}
TiXT	6.7×10^{-14}	2.0×10^{-13}	8.5×10^{-13}
Pure Ti	1.2×10^{-13}	4.8×10^{-13}	1.8×10^{-12}

3.3. Oxide scales analyses

Fig. 3 shows cross-section SEM images of the oxide formed after 1000 h at 600°C for the four alloys and **Table 2** presents the oxide thickness for each alloy at 560°C, 600°C and 650°C. For all alloys, the oxide layer is thicker at 600°C compared to 560°C. At 650°C, the measured oxide thicknesses seem similar to that observed at 600°C, although the mass gain is higher at the highest temperature. This behavior can be explained by the fact that the mass gain is mainly due to the oxygen dissolution into the substrate and not to the formation of the oxide scale [7]. Parabolic rate constants and the oxide thicknesses are similar for Ti6242S and Ti6426 alloy for the three exposure temperatures, as presented in **Table 2**. Variation of molybdenum content from 2% to 6% does not impact on the thickness of the oxide layer.

The oxide thickness on pure titanium is much bigger than on TiXT alloy, confirming that the presence of Si within TiXT alloy increases the high temperature oxidation resistance. This is in accordance with several studies which show that the higher is the content of silicon, the thinner is the oxide layer [16,17]. Chaze *et al.* [16] also demonstrated that the presence of silicon may reduce the porosity of the rutile layer and increase the adherence of the oxide scale, interesting for the protectiveness of the oxide.

SEM and XRD analyses show the formation of TiO_2 rutile which is predominant, and sometimes anatase for all alloys and for each temperature. The presence of 0.45 wt.% of Si in TiXT alloy leads to the formation of Ti_5Si_3 in the underlying substrate after oxidation. This result points out that during oxidation, some Ti atoms react with Si in order to form Ti_5Si_3, preventing the reaction with oxygen, which can contribute to the lower mass gain of TiXT as compared to pure titanium.

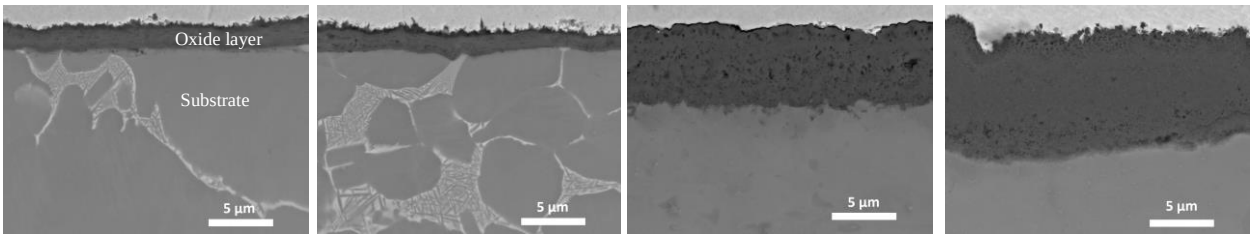

Fig. 3 Cross section SEM images of the oxide layers grown after 1000h of oxidation at 600°C for (a) Ti6242S, (b) Ti6246, (c) TiXT and (d) Pure Titanium

Table 2
Oxide thickness after 1000h of oxidation at 560°C, 600°C and 650°C

	Oxide thickness after 1000h of exposure (µm)		
Alloy	560°C	600°C	650°C
Ti 6242S	0.18 ± 0.02	1.9 ± 0.3	1.7 ± 0.1
Ti 6246	0.16 ± 0.02	1.6 ± 0.3	1.7 ± 0.4
TiXT	1.3 ± 0.2	6.1 ± 0.4	4.9 ± 0.3
Pure Ti	3.7 ± 0.5	7.9 ± 2.2	9.7 ± 0.3

XRD analyses show that, despite the presence of 6 wt.% Al content, Ti6242S and Ti6246 do not present any peak of alumina contrary to what other authors found on TA6V alloy [20]. EDS analyses did not show any variation of aluminum concentration through the oxide scale, probably because of the size of the analyzed zone of the tool (~1 μm^3). However, a darker layer can be seen in the sublayer zone for Ti6242S and Ti6246, and not visible for TiXT and

pure Ti. This probably shows the presence of an Al_2O_3 thin layer which could appear darker in BSE mode. By using XPS analyses, Berthaud *et al*. [7] highlighted a higher amount of aluminum at the external surface of the oxide scale, which means that Al_2O_3 may exist at this location for Ti6242S alloy, while XRD analyses did not show its presence.

To explain the beneficial effect of Si on the oxidation resistance, it is assumed that silicon dissolves as Si^{4+} ions in interstitial positions of the rutile layer. Indeed, the low atomic radius, of about 0,41 Å [16], allows the insertion in the rutile lattice. The presence of Si^{4+} reduces the oxygen diffusion in the rutile and therefore the growth of the layer by decreasing the concentration of oxygen vacancies, which is the main defect in rutile below 900°C. This might explain the lower rate of porosity in the oxide grown at the surface of TiXT as compared to that observed on pure titanium. It is mentioned elsewhere [17] [23] that the presence of Si can form SiO_2 particles finely dispersed in the rutile, which decrease the internal stress, reduce its recrystallization and increase its adherence.

For TiXT, rutile is the main phase in the oxide. EDS analyses reveal no detectable variation of the silicon content in the oxide layer in horizontal and vertical directions, even if Vojtech [23] and Habazaki [24] previously suggested that Si is more concentrated in the inner part of the oxide layer. XRD did not show any peaks of SiO_2, probably because of the small amount of Si contained in the alloy, and/or because SiO_2 can be found in amorphous phase. The unalloyed titanium shows only rutile and anatase after oxidation.

A slightly darker gray layer can be observed for TiXT alloy just below the oxide scale, in the underlying substrate on SEM images (**Fig. 3**), showing that this zone is probably enriched with a light element. Taking into account the high diffusion capacity of nitrogen through rutile layers [25], it can be supposed that this layer is a reaction layer enriched in nitrogen. Such N-rich layer has been also observed for pure Ti by Kanjer *et al.* [26] after 100h of oxidation at 700°C. It has been demonstrated that nitrogen present in the air plays a role in the oxidation resistance. Coddet *et al.* [27] and more recently Torrent *et al.* [28] showed that the presence nitrogen-rich layer reduces the porosity of the oxide layer and increases its adherence, limiting the risk of spallation. Dupressoire *et al.* [8] showed also that the presence of nitrogen in the exposure atmosphere reduces the mass gain after 100h of oxidation of Ti6242S alloy at 650°C.

3.4. Study of the oxygen dissolution zone

Oxygen dissolution in titanium alloys affects the mechanical properties by reducing its ductility. [10,12,21]. Indeed, titanium alloys can dissolve oxygen in its α-phase up to 33% at. in their crystal lattice and up to 4% at. In the β-phase [30]. The oxygen diffusion into a semi-infinite solid can be described by the following equation [19]

$$\frac{C_x - C_0}{C_s - C_0} = 1 - \mathrm{erf}\left(\frac{x}{2\sqrt{Dt}}\right) \qquad \text{eq. 1}$$

where C_x is the oxygen concentration at the depth x, C_0 is the original oxygen concentration of the raw material before oxidation, C_s is the oxygen concentration at the surface, t the time and D is the diffusion coefficient.

Several authors suggest that a linear relationship exists between the oxygen concentration and the hardness of Ti alloys [29,30]. Berthaud *et al* [6,7] also observed that the oxygen content and the hardness of the oxygen-enriched area tend to follow the same profile for oxidation of 1000h up to 10 000h at 560°C of Ti6242S alloy.

However, other authors assume that the correlation between oxygen concentration and the hardness values is better described with a parabolic relationship instead of a linear relationship. This assumption is based on comparisons between these two quantities by Brown, Folkman and Schussler after the study of 152 batches of titanium sponges [32], and then used by Liu and Welsh [33] and by Leyens and Peters [34]. Taking these data into account, Vaché *et al.* [35] recently proposed a new model to estimate more accurately the coefficient of diffusion for oxygen with hardness profiles.

Therefore, in order to estimate the extent of the oxygen dissolution zone, called α-case by some authors, microhardness tests were carried out. Since the hardness depends on the oxygen content by a parabolic relationship, the hardness profile can be described by the following model, proposed by Vaché *et al.* [35]*:*

$$\frac{HV_x - HV_0}{HV_s - HV_0} = \sqrt{1 - \mathrm{erf}\left(\frac{x}{2\sqrt{Dt}}\right)} \qquad \text{eq. 2}$$

where HV_x is the hardness value at the depth x, HV_s is the hardness value at the oxide/metal interface, HV_0 is the hardness value of the bulk material, D is the diffusion coefficient of oxygen in titanium and t is the time. The coefficient D can be calculated by fitting the experimental points with a complementary error function by the least squared method. Then, the oxygen diffusion zone is evaluated by the relation: $L_{diff} = 4\sqrt{Dt}$ as also used by Casadebaigt *et al.* [37], corresponding in this study to the depth where the value of HV_x tends to equal HV_0. **Fig. 4a** presents an example of hardness profile for Ti6242S at 650°C after 1000h of exposure with experimental data and the fitted curve, and **4b** is an example of the evolution of the oxygen dissolution zone at 650°C.

Table 3 presents the diffusion coefficients extracted from the fitting and the corresponding extent of the dissolution zone. It can be noticed that the diffusion coefficient for Ti6242S and Ti6246 are very close for the three temperatures. For TiXT, this value is lower than for pure titanium at 600°C, and similar at 560°C and 650°C.

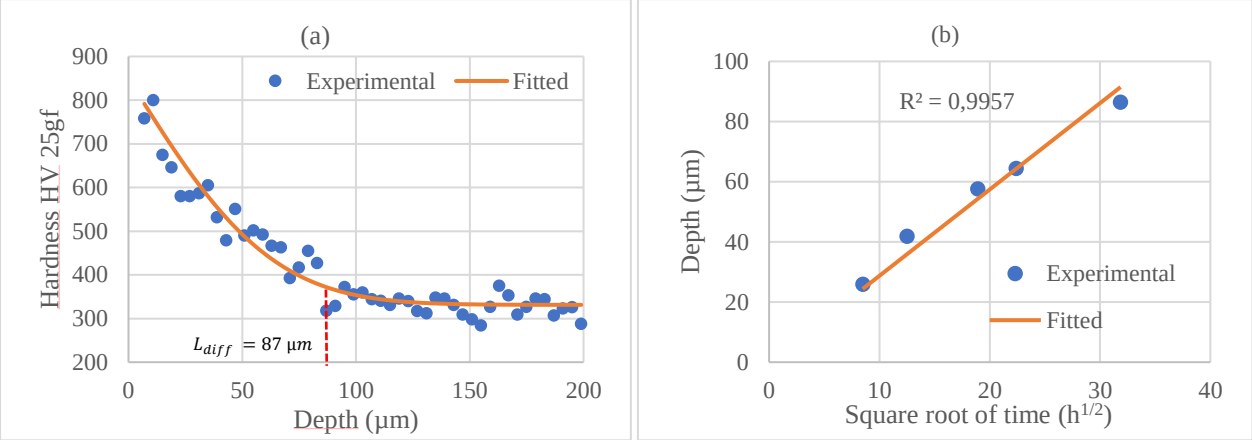

Fig. 4 Example of (a) hardness profile for Ti6242 after 1000h of oxidation et 650°C and (b) evolution of the oxygen dissolution zone versus square root of time at 650°C

Table 3
Coefficients of oxygen diffusion in different Ti alloys and pure Ti diffusion and evolution of oxygen dissolution zone with the oxidation temperature

	Coefficient of diffusion ($m^2.s^{-1}$)			Oxygen dissolution zone after 1000h (µm)		
Alloy	560°C	600°C	650°C	560°C	600°C	650°C
Ti6242S	$(8.7 \pm 3.5) \times 10^{-18}$	$(3.7 \pm 0.4) \times 10^{-17}$	$(1.6 \pm 0.3) \times 10^{-16}$	23	46	95
Ti6246	$(9.8 \pm 3.6) \times 10^{-18}$	$(3.7 \pm 1.2) \times 10^{-17}$	$(1.6 \pm 0.5) \times 10^{-16}$	24	46	95
TiXT	$(9.4 \pm 2.4) \times 10^{-18}$	$(2.8 \pm 0.9) \times 10^{-17}$	$(1.5 \pm 0.2) \times 10^{-16}$	24	40	93
Pure Ti	$(9.9 \pm 1.0) \times 10^{-18}$	$(5.5 \pm 1.5) \times 10^{-17}$	$(1.4 \pm 0.2) \times 10^{-16}$	24	56	90

3.5. Activation energy for the mass gain and for oxygen diffusion

Based on k_p values determined here above, two activation energies can be determined. One is for the total mass gain and the other is for the oxygen diffusion into the substrate. These values are presented in **Table 4**.

The parabolic rate k_p is dependent of the temperature. It can be expressed by an Arrhenius law [19]:

$$k_p = k_0 \exp\left(\frac{-Q_{ox}}{RT}\right) \qquad \text{eq. 3}$$

where k_p is the parabolic rate constant in $g^2.cm^{-4}.s^{-1}$, k_0 is the frequency factor, Q_{ox} is the activation energy for the overall oxidation, R is the universal gas constant (8.3143 $J.mol^{-1}.K^{-1}$) and T the temperature. By plotting the logarithmic values of k_p versus $1/T$, a straight line can be drawn and the slope corresponds to the value of $\left(\frac{-Q_{ox}}{RT}\right)$ and the activation energy can then be estimated. The estimated activation energies are 175 $kJ.mol^{-1}$ and 154 $kJ.mol^{-1}$ for Ti6242S and Ti6246, respectively. For Ti6242S, the values are slightly larger than those found by Gaddam *et al.* [1] and by Shenoy

et al. [4] who estimated these values at 151 kJ.mol^{-1} and 157 kJ.mol^{-1} respectively but lower than 262 KJ.mol^{-1} found by Berthaud [6] and than 245 kJ.mol^{-1} found by Vaché *et al.* [36]. For Ti6246 alloy, the energy activation is slightly lower compared to Ti6242S. For TiXT and Pure Ti, the activation energy is estimated at 181 kJ.mol^{-1} and 191 kJ.mol^{-1}, respectively (See **Table 4**).

The oxygen dissolution coefficient is also dependent of the temperature and expressed by an Arrhenius law [19]:

$$D = D_0 \exp\left(-\frac{Q_{diff}}{RT}\right) \qquad \text{eq. 4}$$

where D is the coefficient of oxygen dissolution, D_0 is the pre-exponential factor, Q_{diff} is the activation energy for oxygen diffusion, R is the universal gas constant (8.3143 J.mol^{-1}.K^{-1}) and T the temperature.
The activation energies for dissolution are estimated at 205 kJ.mol^{-1} for Ti6242S, 197 kJ.mol^{-1} for Ti6246, 198 kJ.mol^{-1} for TiXT and 187 kJ.mol^{-1} for pure titanium (see **Table 5**). No significant differences were found between the couples of alloys. For comparison, the activation energy for oxygen dissolution in Ti6242 was estimated elsewhere at 157 kJ.mol^{-1} [1], 167 kJ.mol^{-1} [4], 198 kJ.mol^{-1} [36], 203 kJ.mol^{-1} [5], 242 kJ.mol^{-1} [3]. For pure titanium, the values were estimated at 191 kJ.mol^{-1} [36] 201 kJ.mol^{-1} [30] and 241 kJ.mol^{-1} [20].
For each alloy, the difference between the activation energy for oxygen dissolution and for overall oxidation process is not high. This could be explained by the fact that, in the temperature range of this study, the oxygen dissolution is prevalent compared to the formation of the oxide scale. Indeed, Berthaud *et al.* [6,7] revealed that the oxygen dissolution represents 79% to 87% of the total mass gain for Ti6242S oxidized at 560°C between 1000h and 10 000h.

Table 4
Activation energy for overall oxidation process and for oxygen dissolution for Ti6242, Ti6246 TiXT and pure Ti in the range of 560°C – 650°C

Alloy	Activation energy for overall oxidation (kJ.mol^{-1})	Activation energy for oxygen dissolution (kJ.mol^{-1})
Ti 6242S	175	205
Ti 6246	154	197
TiXT	181	198
Pure Ti	191	187

Conclusion

The aim of this study was to highlight the effect of Mo and Si in titanium alloys on their high temperature behavior. After isothermal oxidation tests in the range of 560°C – 650°C for 1000h in laboratory air, it was concluded that:

- All the alloys follow a parabolic rate law during the oxidation;
- The oxide layer is mainly composed of rutile. No Al_2O_3 was detected for Al-containing alloys and no SiO_2 was identified despite the presence of Si in the alloys;
- The alloying elements have an important role in the oxidation behavior since the mass gains are substantially lower for the alloys as compared to pure titanium;
- The higher concentration of Mo in Ti6426 alloy as compared to Ti6242 has no effect on the oxidation resistance in the range of 560°C – 650°C;
- The presence of Si in TiXT alloy (Ti-0,45%wt Si) leads to a beneficial effect on the high temperature oxidation behavior by decreasing the mass gains by a factor of 2;
- The activation energy for the overall oxidation process is estimated at 175 kJ.mol^{-1}, 154 kJ.mol^{-1}, 181 kJ.mol^{-1} and 191 kJ.mol^{-1} for Ti6242S, Ti6246, TiXT and pure titanium, respectively;
- The activation energy for oxygen dissolution is estimated at 205 kJ.mol^{-1}, 197 kJ.mol^{-1}, 198 kJ.mol^{-1} and 187 kJ.mol^{-1} for Ti6242S, Ti6246, TiXT and pure titanium, respectively.

Acknowledgements

The authors thank ANR French National Research Agency for financial funding of ALTITUDE project and TIMET Savoie for providing the materials.

References

1. R. Gaddam, B. Sefer, R. Pederson, M.-L. Antti, Mater.Charact.99 (2015) 166–174
2. R. Gaddam, B. Sefer, R. Pederson, M. L. Antti, Sci. Eng. 48 (2013) 1–8

3. K.S. McReynolds, S. Tamirisakandala, Metall. Mater. Trans. A 42 (2011) 1732–1736
4. R.N. Shenoy, J. Unnam, R.K. Clark, Oxid. Met. 26 (1986) 105–124.
5. C.E. Shamblen, T.K. Redden, in: R.I. Jaffee, N.E. Promisel (Eds.), The Science, Technology, and Application of Titanium, Pergamon Press, Oxford, United Kingdom, 1968, pp. 199–208.
6. M. Berthaud, Etude du comportement de l'alliage de titane Ti6242S à haute température sous atmosphères complexes : applications aéronautiques, PhD Thésis Université de Bourgogne Franche-Comté, 2018.
7. M. Berthaud, I. Popa, R. Chassagnon, O. Heintz, J. Lavková, S. Chevalier, Corr. Sci., 164 (2020), 108049
8. C. Dupressoire, A. Rouaix-Vande Put, P. Emile, C. Archambeau-Mirguet, R. Peraldi, D. Monceau, Oxid. Met. 87 (2017) 343–353
9. I. Gurappa, J.Alloy Compd. 389 (2005) 190–197.
10. C. Leyens, M. Peters, W.A. Kaysser, Materials Science Forum Vols. 251-254 (1997) 769-776
11. C. Leyens, M. Peters & W. A. Kaysser, Materials Science and Technology, (1996) 213-218
12. W. Jia, W. Zeng, X. Zhang, Y. Zhou, J. Liu, Q. Wang, J. Mater. Sci. 46 (2011) 1351–1358.
13. B. Champin, L. Graff, M. Armand, G. Béranger, C. Coddet, J. Common Met. 69 (1980) 163–183,
14. A. M. Chaze, C. Coddet et G. Béranger, Journal of the Less-Common Metals. 83 (1982) 49 - 70
15. Julius C. Schuster and Martin Palm Reassessment of the Binary Aluminum-Titanium Phase Diagram Journal of Phase Equilibria and Diffusion 27(2006) 255-277
16. A.M. Chaze and C. Coddet, Oxidation of Metals, Vol 27, Nos. 1/2, 1987
17. K. Maeda, S. Suzuki, K; Ueda, T. Kitashima, S. Kr. Bhattacharya, R. Sahara, T. Narushima, Journal of Alloys and Compounds 776 (2019) 519-528
18. Y. Shida, H. Anada, Mater. Trans. JIM 35 (1994) 623-631.
19. Kofstad, Per. "High temperature corrosion." Elsevier Applied Science Publishers, Crown House, Linton Road, Barking, Essex IG 11 8 JU, UK, 1988. (1988).
20. H.L. Du, P.K. Datta, D.B. Lewis, J.S. Burnell-Gray, Corros. Sci. 36 (1994) 631–642
21. J. Unnam, R.N. Shenoy, R.K. Clark, Oxid. Met. 26 (3/4) (1986) 231–252.
22. Rosa, Casimir J. "Oxidation of Ti-1Si and Ti-5Si alloys." Oxidation of Metals 17(5-6) (1982) 359-369.
23. D. Vojtech, B. Bartova, T. Kubatík, Mater. Sci. Eng. A 361 (2003) 50-57.
24. H. Habazaki, K. Shimizu, S. Nagata, P. Skeldon, G.E. Thompson, G.C. Wood, Corros. Sci. 44 (2002) 1047.
25. A.M. Chaze and C. Coddet, The role of nitrogen in the oxidation behaviour of titanium and some binary alloys, Journal of the Less-Common Metals, 124 (1986) 73 – 84.
26. A. Kanjer, L. Lavisse, V. Optasanu, P. Berger, C. Gorny, P. Peyre, F. Herbst, O. Heintz, N. Geoffroy, T. Montesin, M.C. Marco de Lucas, Effect of laser shock peening on the high temperature oxidation resistance of titanium Surf. Coat. Technol., 326 (2017) 146-155
27. C. Coddet, A.M. Chaze, The role of nitrogen in the oxidation behaviour of titanium and some binary alloys, Journal of The Less Common Metals, 124 (1986) 73-84
28. F. Torrent, L. Lavisse, P. Berger, G. Pillon, C. Lopes, F. Vaz, M.C. Marco de Lucas, Influence of the composition of titanium oxynitride layers on the fretting behavior of functionalized titanium substrates: PVD films versus surface laser treatments Surf. Coat. Technol., 255 (2014) 146-152
29. K.N. Strafford and J.M. Towell, The Interaction of Titanium and Titanium Alloys with Nitrogen at Elevated Temperatures. I. The Kinetics and Mechanism of the Titanium-Nitrogen Reaction, Oxidation of Metals, Vol. 10, No. 1, 1976, 41-67
30. Rosa, Casimir J. Metallurgical Transactions 1(9) (1970) 2517-2522.
31. M. Göbel, V.A.C. Haanappel, M. F. Stroosnijder, On the Determination of Diffusion Coefficients of Oxygen in One-Phase Ti (α-Ti) and Two-Phase Ti–4Nb (α- and β -Ti) by Micro-Hardness Measurements, Oxidation of Metals, Vol. 55 (2001), 137-151
32. H. Conrad, Progress in Materials Science 26, 123 (1981).
33. Z. Liu and G. Welsch, Metallurgical Transactions A 19, 527 (1998).
34. C. Leyens and M. Peters (eds.), Titanium and Titanium Alloys: Fundamentals and Applications, 1st edn. (Wiley, New York, 2003).
35. N.Vaché, D.Monceau, Oxygen Diffusion Modeling in Titanium Alloys: NewElements on the Analysis of Microhardness Profiles, Oxidation of Metals (2020) 93:215–227
36. N. Vaché, Y. Cadoret, B. Dod, D. Monceau, Modeling the oxidation kinetics of titanium alloys: Review, method and application to Ti-64 and Ti-6242s alloys, Corrosion Science 178 (2021) 109041
37. A.Casadebaigt, D.Monceau, J.Hugues, High Temperature Oxidation of Ti-6Al-4V Alloy Fabricated by Additive Manufacturing. Influence on Mechanical Properties, MATEC Web of Conferences 321, 03006 (2020)